Available online at www.sciencedirect.com
ScienceDirect
Nuclear Physics B Proceedings Supplement 00 (2018) 1–6
Nuclear Physics B Proceedings Supplement

Using reference stars for verification of the end-to-end absolute calibration and the long term monitoring of the Fluorescence Detector of the Pierre Auger Observatory

A. Segreto[a,b,*], for the Pierre Auger Collaboration[c,**]

[a] *INAF/IASF, Via Ugo La Malfa 153, 90146 Palermo, Italy*
[b] *INFN, Via Santa Sofia 64, 95123 Catania, Italy*
[c] *Observatorio Pierre Auger, Av. San Martín Norte 304, 5613 Malargüe, Argentina*

Abstract

The absolute calibration of the fluorescence detector telescopes of the Pierre Auger Observatory is an important element for correctly determining the energy of primary cosmic rays producing extensive air showers in the atmosphere. In this contribution we show that signals generated by stars traversing the field of view of the fluorescence detectors can effectively be used as a tool to verify their absolute calibration without requiring any dedicated external hardware device. After describing the details of the procedure we report on the preliminary results obtained by the analysis of signals from reference stars as observed by the fluorescence detector telescopes.

Keywords: Pierre Auger Observatory, fluorescence telescope, calibration, long term monitoring

1. Introduction

The Pierre Auger Observatory [1] located in Malargüe, Argentina, employs several Fluorescence Detector (FD) telescopes to obtain calorimetric estimates of air shower energies generated by primary cosmic rays. Absolute end-to-end calibration of these telescopes is obtained by means of an absolutely calibrated pulsed light-source (Drum) [2], temporarily mounted on the outside of the telescope aperture. Moreover, to monitor the gains of PMTs, a permanently-installed light source directly illuminates the telescope camera [3] at the beginning and at the end of each data taking period.

The overall telescope response, however, may evolve in time under the influence of several factors (such as accumulation of dust on the mirrors and filters) that cannot be monitored by the implemented relative calibration system. To provide an independent verification and a long-term monitoring of the FD absolute-calibration status, a procedure has been developed based on the analysis of the signals generated by reference stars crossing the field of view of the FD telescopes.

Photometry of standard stars is a method commonly used for the calibration of optical telescopes, however, the fluorescence telescopes (designed to detect very short burst of light) are not able to directly record the slowly-varying photon flux generated by stars. Nevertheless, it is possible, to obtain, from the statistical fluctuations (variance) of the detected signals, an indirect measure of the photon flux illuminating the telescopes. Without requiring any dedicated hardware device, and without any interference with the normal telescope operations, analysis of the signals induced by reference stars could then provide an alternative way to verify and monitor the FD absolute calibration, independently from other methods based on the use of pulsed artificial sources.

In this contribution we describe in detail the procedure to analyze the star signals observed by the FD tele-

*e-mail: segreto@ifc.inaf.it
**Full author list: http://www.auger.org/archive/authors_2018_06.html

scopes, in particular the correction of the atmospheric attenuation, and show a few examples of data analysis on reference stars.

2. The FD telescopes

At the Pierre Auger Observatory, several FD telescopes (having a field of view $30^\circ \times 30^\circ$) are situated along the external perimeter of the Observatory in four separated sites: Los Leones, Los Morados, Loma Amarilla and Coihueco; in each of these sites, 6 telescopes are installed in adjacent bays covering a total azimuth range of 180° and pointing to the sky at $\approx 15^\circ$degrees of elevation angle; moreover, three additional telescopes named HEAT (High Elevation Auger Telescopes), pointing to the sky at $\approx 45^\circ$ elevation angle, are located at the Coihueco site.

The camera of each FD telescope consists of 440 hexagonal photo-multipliers, which are organized in honeycomb-like structure having 22 rows and 20 columns. Besides recording the full ADC traces of the signals relative to the PMTs illuminated by cosmic ray showers, the acquisition software of the FD telescopes continuously computes, for every camera pixel, the average and the statistical variance of the PMT signals [4], recording the results at periodic intervals (usually every 30 s, reduced to 5 s when required). From the variance data, after subtraction of the dark and electronic noise, a map representing the night-sky background flux in the field of view of the FD telescopes can be recovered.

The strict proportionality between the FD variance and the night-sky background flux has been verified by means of a small calibrated detector, UVscope [5], placed on top of one of the FD buildings. The excellent agreement [6] between the absolute background night-sky flux as measured (in single-photon counting mode) by UVscope and the value reconstructed from the FD variance data, indicates that the absolute flux of the stars in field of view of the FD telescopes can be accurately determined and, therefore, that observations of reference stars could be used to verify the FD-telescope calibration status. Of course a fundamental part of the calibration method is to accurately correct the measured star signal for the strong atmospheric attenuation, as FD telescopes may only observe stars at low elevation angles.

3. Atmospheric attenuation

As it passes through the atmosphere, the star light is attenuated by scattering and absorption. In the wavelength range (300 to 400 nm) where the FD telescopes are sensitive, the light attenuation (atmospheric extinction) is due to three different physical processes: Mie scattering from aerosols (particles with physical size on the order of the wavelength of light), scattering from the air molecules themselves (Rayleigh scattering) and absorption in the ozone layer.

In Fig. 1 we plot a typical vertical atmospheric transmission as a function of wavelength, with the contribution of the three physical processes shown separately.

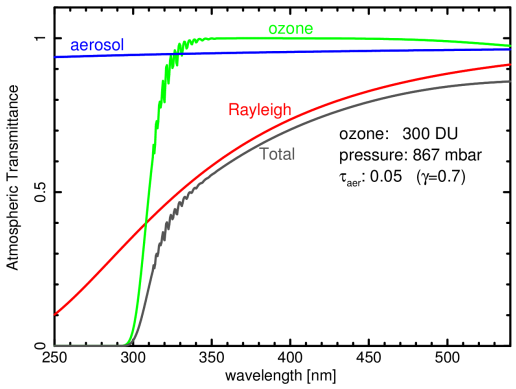

Figure 1: The typical wavelength dependence of the atmosphere transmission with the contribution of three physical process shown separately.

As evident from the plot, there is a strong wavelength dependence of the total atmospheric transmission due to the Rayleigh scattering and, below 320 nm, due to the absorption in the ozone layer. The Mie scattering from the aerosol particles is apparently the least important, however, its contribution to the atmospheric extinction is by far the most problematic to estimate since the aerosol concentration is highly variable, in unpredictable way, from night to night, and can also change in a significant way during the night.

3.1. Atmospheric attenuation vs. star position

The total attenuation of the star light depends on the length of the path that the light follows in its propagation through the atmosphere and, therefore, from the star elevation angle. This dependence is usually expressed as a function of the air-mass factor, defined as the ratio of the optical path corresponding to the actual star position to the optical path along the vertical (the air-mass factor is, therefore, equal to one when a star is observed at the zenith).

If the Earth's curvature is ignored, the air mass-factor, X, is simply expressed by the secant of the star zenith angle z,

$$X(z) \approx \frac{1}{\cos(z)}, \tag{1}$$

however, when observing a star at low elevation angles ($\lesssim 30^\circ$) the Earth's curvature must necessarily be taken into account and more precise and complex formula must be used.

The air-mass factor allows us to express the total atmosphere transmission as a function of the position at which the star is observed,

$$T_{\rm atm}(\lambda, z) = \exp\left[-\tau_{\rm atm}\,(\lambda)\; X(z)\right] \qquad (2)$$

where $\tau_{\rm atm}\,(\lambda)$ is the total optical depth of the atmosphere, corresponding to a vertical path.

3.2. Telescope signal vs. star position

The measured star signal actually depends on the telescope spectral response and on the spectral distribution of the star light reaching the telescope (which depends on the atmospheric extinction) and can be expressed in general with:

$$S\,(z) = K_{\rm abs} \int_0^\infty \varepsilon_{\rm tel}\,(\lambda)\; T_{\rm atm}(\lambda, z)\, \Phi_{\rm star}\,(\lambda)\; {\rm d}\lambda \qquad (3)$$

where $\Phi_{\rm star}\,(\lambda)$ is the star spectral-flux density as would be observed on top of the Earth's atmosphere, $T_{\rm atm}\,(\lambda, z)$ the total atmospheric transmissivity, $\varepsilon_{\rm tel}\,(\lambda)$ is the telescope spectral response (including sensor quantum efficiency, mirror reflectivity, filter transmission, etc.) and $K_{\rm abs}$ is the absolute calibration constant that takes into account the telescope geometry and any other factor (e.g. electronic gain) independent from wavelength.

Assuming that within the telescope sensitive region it is possible to neglect the wavelength dependence of the atmospheric transmission, Eq. (3) can be approximated as

$$S\;(z) \approx K_{\rm abs}\, e^{-\bar{\tau}_{\rm atm}\, X(z)} \int_0^\infty \varepsilon_{\rm tel}\,(\lambda)\; \Phi_{\rm star}\,(\lambda)\; {\rm d}\lambda \qquad (4)$$

where $\bar{\tau}_{\rm atm}$ is the average aerosol optical-depth in the telescope sensitive region.

By taking the logarithm of the above equation, a linear relation known as Bear-Lambert-Bouguer equation is obtained,

$$\ln\,(S\,) = \ln\,(S_0) - \bar{\tau}_{\rm atm}\, X, \qquad (5)$$

where

$$S_0 = K_{\rm abs} \int_0^\infty \varepsilon_{\rm tel}\,(\lambda)\; \Phi_{\rm star}\,(\lambda)\; {\rm d}\lambda. \qquad (6)$$

According to Eq. (5), if the logarithms of the star signals measured at different zenith angles are represented versus the air-mass factor (the so called Langley plot) the data are aligned along a straight line whose slope depends only on the atmospheric optical thickness and whose extrapolation at $X = 0$ provides the signal S_0 that would be measured in absence of the atmosphere.

It is important to stress, however, that for telescopes sensitive in a wide wavelength range, the strong wavelength dependence of the atmospheric transmission cannot be neglected and therefore Eq. (5) becomes not accurate. In these cases, the proper way to determine S_0 is to perform a parametric fit to the data by directly using the exact relation provided by Eq. (3).

4. Reference standard stars

To verify the absolute calibration of a telescope it is necessary to observe a bright star with a very stable luminosity and whose spectral distribution has been accurately calibrated.

The star usually used as primary reference for absolute astronomical photometry is Vega (α Lyr) [7], but in the southern hemisphere Sirius (α CMa) is preferred since it can be observed at higher elevation angles (therefore with lower atmospheric attenuation). Both of these sources have been observed, free of any atmospheric contamination, by the Space Telescope Imaging Spectrograph (STIS) on board the Hubble Space Telescope. The absolutely calibrated spectra of these two sources, having a spectral resolution of 0.25 nm and an absolute uncertainty of 1%, are shown in Fig. 2.

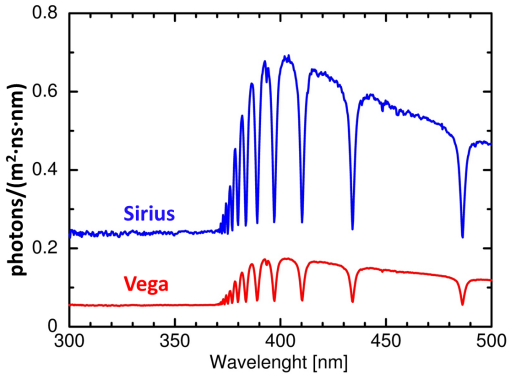

Figure 2: The absolutely calibrated (0.25 nm resolution, 1% uncertainty) spectral distribution of two reference stars, Vega and Sirius, as measured outside the Earth's atmosphere.

Due to the wavelength dependence of the atmospheric extinction, the spectral distribution of the star

light reaching the telescope depends significantly on the altitude at which the star is observed. In Fig. 3 we show the Sirius spectrum multiplied by the spectral response of the FD telescopes and by the atmospheric transmission relative to star observations at 60° and 15° elevation angle.

As evident, the shape of the spectral distribution of detected photons is a function of the star altitude, and the detector signal, which is proportional to the area under the curves, can be computed by numerical integration of Eq. (3).

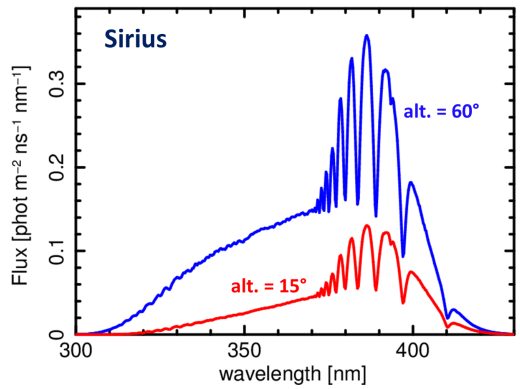

Figure 3: The spectral distribution of photons which contribute to the FD telescope signal when Sirius is observed at two different altitudes. The shape of the two spectral distributions is different because of the significant wavelength dependence of the atmospheric extinction. The detector signal is proportional to the area under the curves.

5. The analysis of FD star signals

A star becomes visible at night-time by two or more FD telescopes for a few months per year, and always follows the same path within the telescope field of view (apart for the long-term drift due to the astronomical precession). In Fig. 4, we show the path of Sirius across the field-of-view of the FD telescope situated in the bay 6 at the Loma Amarilla site.

In the following paragraph we illustrate an example of FD data analysis on this star, which is performed by comparing the signal measured by the telescope, as a function of the star position, to the expected signal as obtained from Eq. (3).

5.1. The measured star flux

After selection from the FD archive of the data relative to cloudless nights and subtraction for the diffuse component of the night-sky-background, we convert the ADC variance to physical photon-flux units following the method described in [6]. We then add the contribution of the three camera pixels whose pointing direction

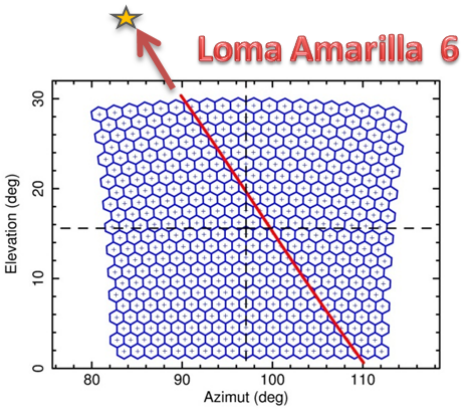

Figure 4: Visualization of sky trajectories of Sirius crossing the field of view of telescope located in Loma Amarilla bay 6; the hexagonal field of view of each camera pixels is also shown.

is closest to the position of the reference star, thus obtaining the total star flux along the path in the field of view of the telescope.

It is also important to take into account the fact that when a star moves across the field of view of the FD telescope, the measured flux is modulated by the spatial variation of the efficiency (due to the nonuniform sensitivity of PMTs and reduced collection efficiency) at the boundary between adjacent pixels. In order to correct for this effect, a correction map has been obtained, by means of an analytic model, reproducing the modulation caused by the hexagonal pattern of the camera.

5.2. The expected star flux

Assuming that both the spectrum of the observed star and the spectral response of the FD telescope [8] are known, to compute the expected star signal it is necessary to determine the atmospheric extinction during the selected night.

We can determine the amount of Rayleigh scattering from the local barometric pressure and retrieve from public archives (where measurements performed by dedicated satellites are stored) the total optical thickness of the ozone layer above the Observatory. The only unknown parameter for a full modeling of the atmosphere extinction is therefore the aerosol optical thickness.

We then initially exclude the aerosol optical-depth from the atmospheric extinction model and compare, on a Langley plot, the signal obtained from Eq. (3) to the signal actually measured by the telescope. In Fig. 5, a typical plot obtained is shown. The different slopes of the two curves are proportional to the

aerosol optical-depth not yet included in the atmospheric model. The undulation in the curves is due to the detection-efficiency loss when the star transits between adjacent camera pixels.

By fitting the ratio between measured and simulated flux (shown in the lower panel of Fig. 5) we obtain the actual aerosol optical-depth and a multiplicative scaling factor to correct for the curve normalization.

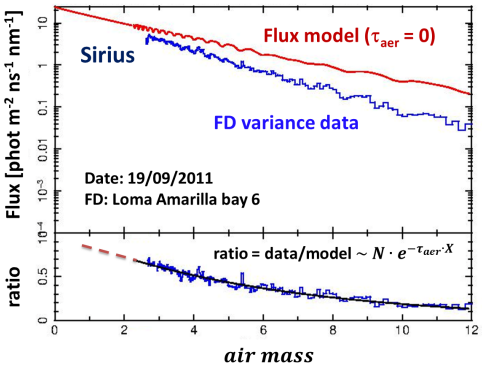

Figure 5: Initial comparison, on a Langley plot, between the flux of Sirius as obtained from the variance data recorded by the FD telescope in Loma Amarilla bay 6 during the night 19/09/2011, and the expected star signal, computed without including the aerosol optical depth in the atmospheric extinction model. The slope of the measured flux, significantly higher than the slope of the simulated data, clearly indicates the necessity to add the aerosol effects in the atmospheric model.

The procedure is then repeated, adjusting both the aerosol-optical depth and normalization factor until a good match, like the one shown in Fig. 6, between the two curves is obtained. Of course, in case of a well calibrated telescope, the normalization factor is expected to be equal to one within statistical errors.

5.3. *Example of star observed in different aerosol conditions*

As a further example of the effectiveness of the method adopted to correct the star-flux measurement from the atmospheric extinction, we show in Fig. 7 the results obtained from the analysis of data relative to Sirius as observed during two nights characterized by very different aerosol optical-depths.

While the star-flux measurements between the two nights are significantly different, the extrapolations of the two curves at $X = 0$ meet in the same point, thus indicating that the telescope calibration status was indeed the same during these two nights.

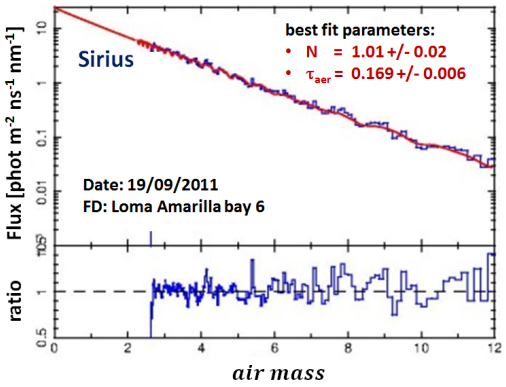

Figure 6: Comparison between the Sirius flux measured by the FD telescope in Loma Amarilla bay 6 during the night 19/09/2011, and the simulated flux, after an iterative fitting procedure in which the aerosol-optical depth and a normalization factor are the only parameters allowed to vary.

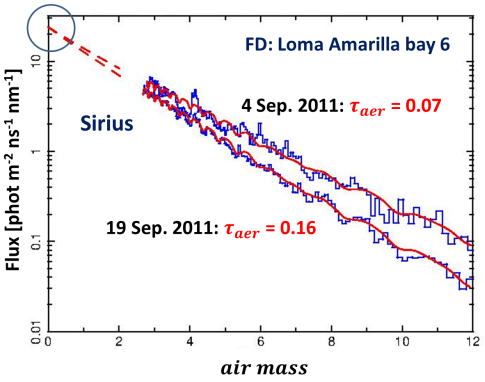

Figure 7: Sirius flux vs. air mass observed in two nights with different aerosol-optical depths. Although the data have different slopes, their extrapolations at $X = 0$ meet at the same point, indicating a consistent value for the absolute telescope calibration.

.

5.4. *Analysis of other reference stars*

Besides Sirius, many other bright stars can be used as a reference to monitor the FD calibration status. For example, in Fig. 8, we show the data analysis results relative to three stars, Sirius, Rigel and Saiph, as observed by the selected FD telescope during the the same night (at different times).

As is evident, for all the three stars, the agreement between the expected and measured signal is quite good over almost four orders of magnitude in flux intensity.

Further examples of application of the method we have developed can be found in [9].

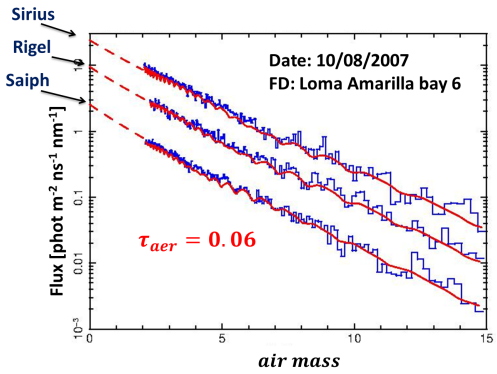

Figure 8: Data from three stars observed by the FD telescope located in bay 6 at Loma Amarilla site during the night of 10/08/2007. The stars, having different magnitudes and spectral shapes, cross the field of view of the telescope in different regions and at different times. In all three cases, the measured data are fully consistent with the expected values (red continuous line).

6. Conclusion

In this work we have demonstrated that the star signals, extracted from the FD variance data, can be used as an independent tool to verify the absolute calibration of these telescopes.

As result of the first analysis on a few reference stars, we have found that absolute fluxes measured by the FDs are in a good agreement with the one expected, confirming the good calibration status of the telescopes.

Main advantage of the developed method is that it allows to monitor the telescope calibration status on a very long time-scale without requiring any external device. Moreover, by star observations it is possible to easily verify the inter-calibration status of telescopes pointing in the same direction, but placed in different locations, as the telescopes are simultaneously illuminated by the same light flux, a condition that cannot be obtained by means of artificial light sources placed at finite distance.

The results obtained at the Pierre Auger Observatory establish the validity of the method which is however quite general and can be therefore adopted to verify the absolute calibration of any other kind of telescopes (like e.g. the Imaging Atmospheric Cerenkov Telescopes) not able to directly record the star light.

References

[1] The Pierre Auger Collaboration, The Pierre Auger Cosmic Ray Observatory, Nuclear Instruments and Methods in Physics Research A 798 (2015) 172–213.

[2] J. T. Brack, R. Cope, A. Dorofeev, B. Gookin, J. L. Harton, Y. Petrov, A. C. Rovero, Absolute calibration of a large-diameter light source, Journal of Instrumentation 8 (2013) P05014.

[3] G. Salina, Pierre Auger Collaboration, Automated procedures for the Fluorescence Detector calibration at the Pierre Auger Observatory, in: 34th International Cosmic Ray Conference (ICRC2015), Vol. 34, 2015, p. 594.

[4] M. Kleifges, A. Menshikov, D. Tcherniakhovski, H. Gemmeke, Statistical current monitor for the cosmic ray experiment pierre auger, IEEE Transactions on Nuclear Science 50 (2003) 1204–1207.

[5] M. C. Maccarone, O. Catalano, S. Giarrusso, G. La Rosa, A. Segreto, G. Agnetta, B. Biondo, A. Mangano, F. Russo, S. Billotta, Performance and applications of the UVscope instrument, Nuclear Instruments and Methods in Physics Research A 659 (2011) 569–578.

[6] A. Segreto, Night Sky Background measurements by the Pierre Auger Fluorescence Detectors and comparison with simultaneous data from the UVscope instrument., in: 32th International Cosmic Ray Conference (ICRC2011), Vol. 3, 2011, p. 129.

[7] C. Megessier, Accuracy of the astrophysical absolute flux calibrations: visible and near-infrared., Astronomy and Astrophysics 296 (1995) 771.

[8] A. C. Rovero, P. Bauleo, J. T. Brack, J. L. Harton, R. Knapik, the Pierre Auger Collaboration, Multi-wavelength calibration procedure for the pierre Auger Observatory Fluorescence Detectors, Astroparticle Physics 31 (2009) 305–311.

[9] P. H. Nguyen, Energy systematics and long term performance of the pierre auger observatory's fluorescence telescopes, Ph.D. thesis, School of Chemistry and Physics : Physics (1998).